Supporting Information

A Cyclophane-Based Host–Guest Charge Transfer Complex for NIR-II Photothermal Conversion

Fei Yang,[a] Yunong Li,[a] Kecheng Huang,[a] Wei Wei[*b] and Yanqing Xu[*a]

[a] Key Laboratory of Medical Molecule Science and Pharmaceutical Engineering, Ministry of Industry and Information Technology, School of Chemistry and Chemical Engineering, Beijing Institute of Technology, Beijing 100081, China. E-mail: xyq@bit.edu.cn

[b] Beijing Key Laboratory for Optical Materials and Photonic Devices, Department of Chemistry, Capital Normal University, Beijing 100048, China. E-mail: wwei@cnu.edu.cn

Table of Contents

1. Method and Synthesis

1.1 General method

All the reagents involved in this research were commercially available and used without further purification unless otherwise noted. ^{1}H and ^{13}C NMR spectra were recorded on a Bruker AVANCE III 400 spectrometer. All chemical shifts are reported in ppm with residual solvents or TMS (tetramethylsilane) as the internal standards. High-resolution electrospray-ionization mass spectrometry (HRMS) experiments were conducted on a Thermo Fisher Q Exactive mass spectrometer. UV-vis-NIR spectroscopy studies were performed on a Shimadzu UV-2550 spectrophotometer. DSC measurements were performed on a Shimadzu DSC-60 machine. 1064 nm NIR laser (MDL-III-1064-2.5W) was purchased from Changchun New Industries Optoelectronics Technology Co., Ltd. Thermal imaging was recorded by FOTRIC 326C camera. The synthesis of **TBox-1^{2+}** has been reported earlier.[S1]

1.2 Synthesis of TBox-1^{2+}
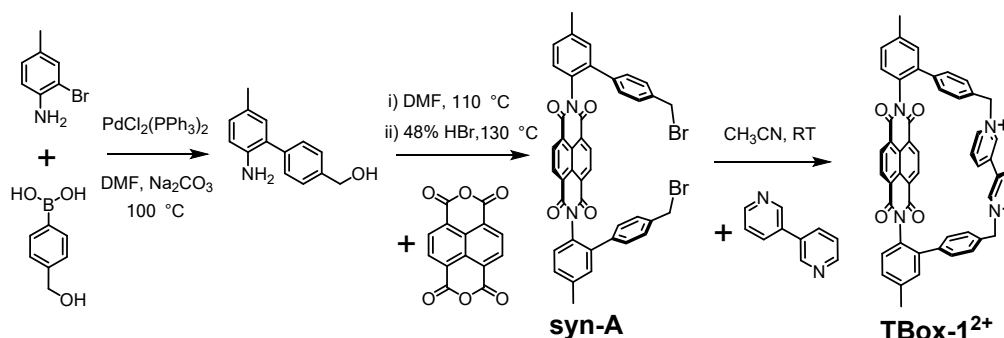
Scheme S1. The synthetic route of **TBox-1^{2+}**.[S1]

1.3 Preparation of TTF⊂TBox-1^{2+}

Excess **TTF** was added to **TBox-1·2Cl** aqueous solution, and then the mixture was sonicated about 30 min. After that, the **TTF⊂TBox-1^{2+}** solution was collected by vacuum filtration. Mixing the aqueous solutions of **TTF⊂TBox-1^{2+}** and NH$_4$PF$_6$, the formed precipitate was washed with water and then dried to afford **TTF⊂TBox-1^{2+}** powders.

1.4 UV-vis titration

For the UV-vis titration experiments, when the solution of guest **TTF** was added incrementally to the solution of **TBox-1^{2+}**, the UV-vis spectra were recorded one after the other. The stacked spectra show that, upon the addition of guest, new absorption bands emerge and

are enhanced. The nonlinear curve-fitting method was then used to obtain the association constant through the following equation:

$$\Delta A = \Delta\varepsilon * \{0.5*G_0 + 0.5*(H_0 + 1/K_a) - \text{sqrt}[0.25*(H_0 + G_0 + 1/K_a)^2 - H_0*G_0]\}$$

where ΔA is the change in the absorbance on gradual addition of guest **TTF**, whereas $\Delta\varepsilon$ refers to the difference of molar absorptivity between host-guest complexes and free hosts; the total concentration of **TBox-1^{2+}** and **TTF** is denoted by H_0 and G_0. From the UV-vis titration experiments, plots of absorption intensity against the guest concentrations were obtained and nonlinear least squares data treatments (red line) gave the corresponding association constants of host-guest complexes.[S2]

1.5 Photothermal performance test

TTF⊂TBox-1^{2+} solution were put in a quartz cuvette and **TTF⊂TBox-1^{2+}** powders were put on quartz glass. A 1064 nm NIR laser (MDL-III-1064-2.5W, Changchun New Industries Optoelectronics Technology Co., Ltd, China) was used to study the photothermal conversion performance of **TTF⊂TBox-1^{2+}**. And the temperature was measured with an IR thermal camera (FOTRIC 326C). The calculation of photothermal conversion efficiency was determined according to previous methods.

1.6 Preparation of bacterial solutions

A single colony of *E. coli* on a solid Luria-Bertani (LB) agar plate was transferred to 15 mL of liquid LB culture medium and was grown at 37 °C for 6 h. Then bacteria were washed with PBS, centrifugated (5000 rpm, 3 min) for 3 times, and resuspended in PBS at OD_{600} of ~ 1.2.

1.7 Antibacterial activity assessment of TTF⊂TBox-1^{2+}

40 μL of *E. coli* suspension ($OD_{600} \approx 1.2$) was incubated with 260 μL **TTF⊂TBox-1^{2+}** solution (0.30 mM) for 5 min. Then, two sets of the *E. coli* suspensions which have been treated with **TTF⊂TBox-1^{2+}** solution were kept in the dark or irradiated by a 1064 nm NIR laser 15 min. Finally, all of the *E. coli* suspensions were serially diluted 1×10^5 fold with PBS. A 100 μL portion of the dilution with bacteria was spread on the solid LB agar plate, and the colonies formed after 14-16 h incubation at 37 °C were counted. All the experiments were performed in triplicate. The live bacteria ratio was determined by calculating the number of

colony-forming units (CFU). The CFU ratio was calculated according to the following equation (e):

$$CFU\ Ratio = \frac{C}{C_0} \times 100\%$$

(e)

C is the CFU of the experimental group treated with **TTF⊂TBox-1²⁺** under NIR irradiation, and C_0 is the CFU of the control group without any treatments **TTF⊂TBox-1²⁺** and NIR irradiation.

1.8 Solar water evaporation

For photothermal water evaporation performance testing, **TTF⊂TBox-1²⁺** powders (40 mg) are put on polytetrafluoroethylene microfiltration membrane (Φ = 25 mm) tightly. DI water was placed in a glass beaker and the microfiltration membrane with the **TTF⊂TBox-1²⁺** powders was put and self-floated on the top of water. The sun solar light irradiation (2500 W m⁻²) was illuminated from the top and onto the surface of the **TTF⊂TBox-1²⁺** powders vertically. The temperature of the **TTF⊂TBox-1²⁺** powders was recorded by IR camera and The weight loss of water was measured by an electronic mass balance.
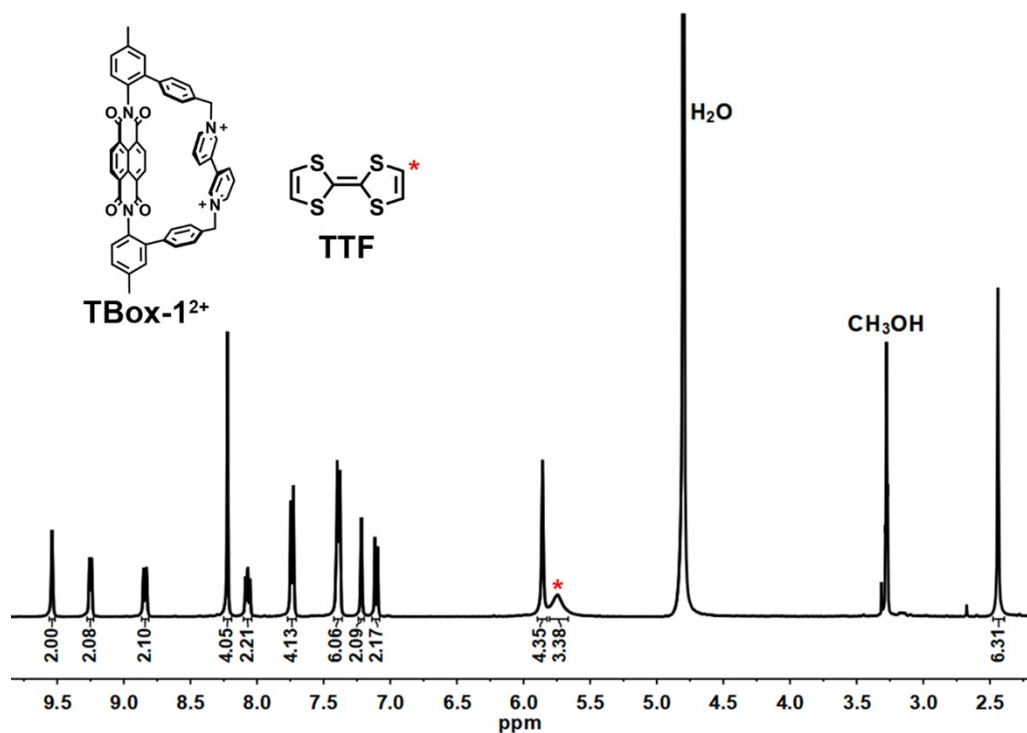
2. Characterization of Host-Guest Properties

Fig. S1. Partial ^{1}H NMR spectrum of **TTF⊂TBox-1^{2+}** in D$_2$O. The integral area of the host/guest NMR resonance shows 1:1 host-guest stoichiometry.
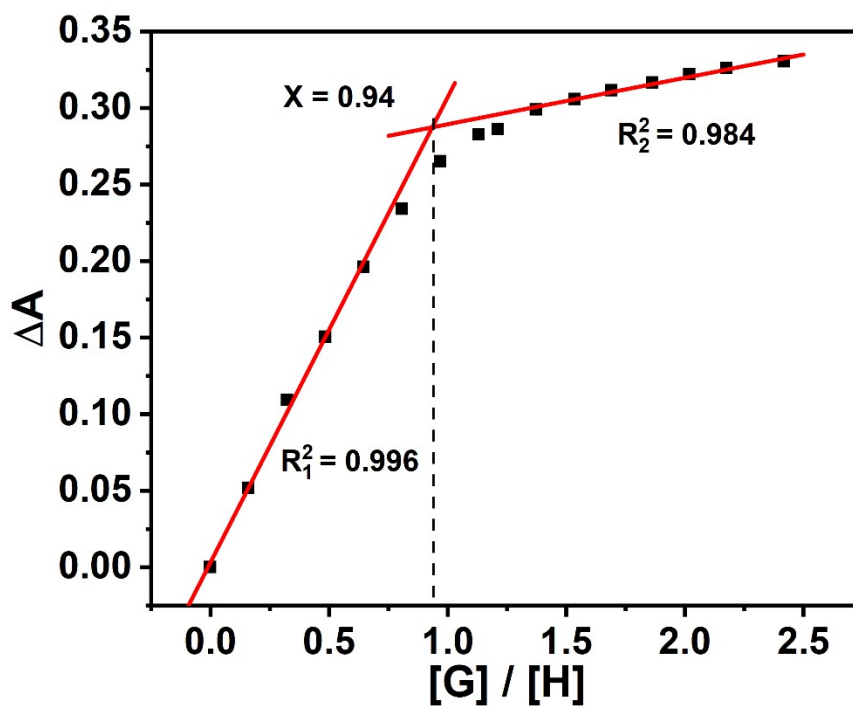

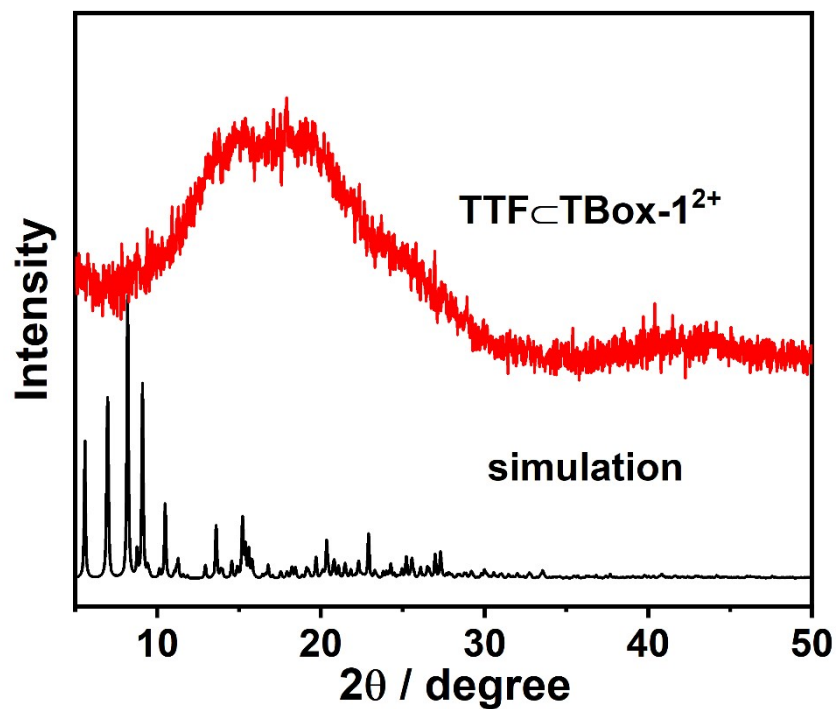**Fig. S2.** Mole ratio for **TBox-1^{2+}** and **TTF**, indicating a 1:1 host-guest stoichiometry.

Fig. S3. PXRD characterization of **TTF⊂TBox-1²⁺**.
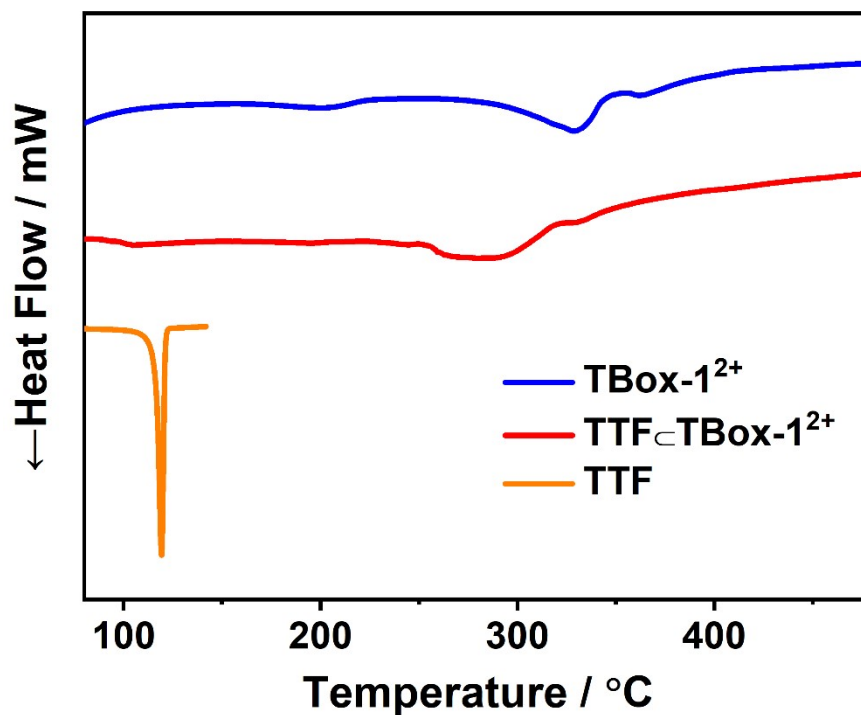
Fig. S4. DSC spectrum of **TBox-1²⁺**, **TTF** and **TTF⊂TBox-1²⁺**.
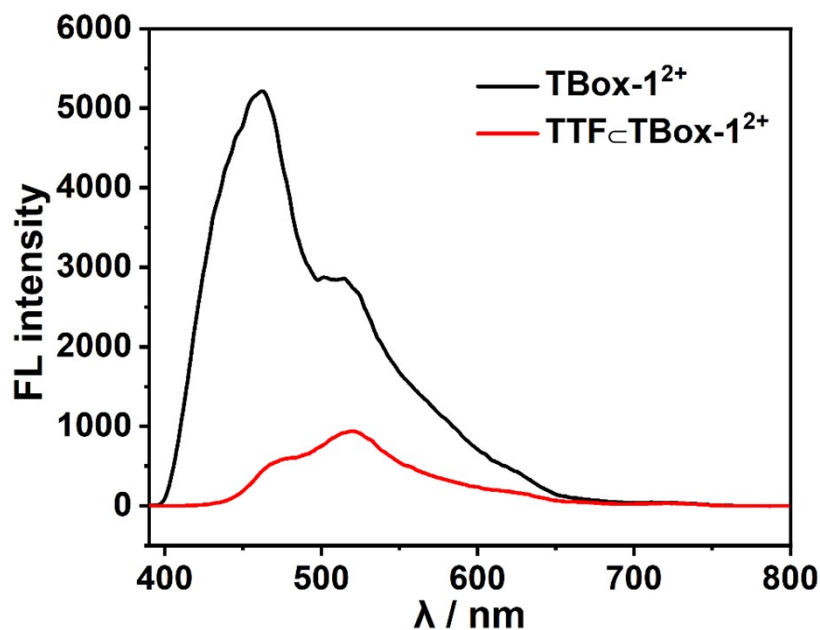
Fig. S5. Fluorescence spectra of **TBox-1^{2+}** and **TTF⊂TBox-1^{2+}** solution, λ_{ex} = 385 nm.
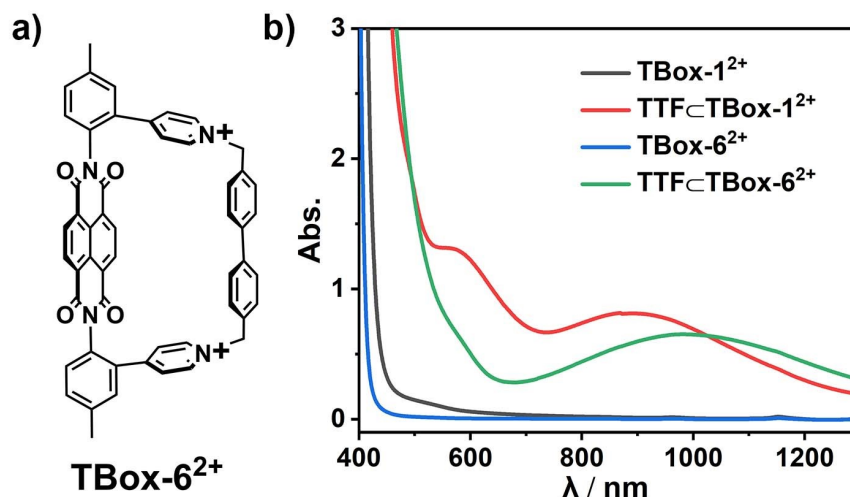
Fig. S6. (a) Chemical structures of **TBox-6^{2+}**[S3]. (b) UV-vis-NIR spectra obtained by adding **TTF** into aqueous solution of **TBox-1^{2+}** and **TBox-6^{2+}** at 298 K.

As shown in Fig. S6, **TBox-6^{2+}** is comprised of NDI and biphenyl moieties as side walls, without 3,3'-bipyridinium group. For **TTF⊂TBox-6^{2+}**, the broad absorption band from 700 to 1300 nm also existed, but there was no absorption at around 574 nm. Therefore, it is reasonable to conclude that the NIR band can be due to the CT interaction between **TTF** and NDI moieties, while the absorption band at 574 nm in tile compound **TTF⊂TBox-1^{2+}** is ascribed to the CT effect between **TTF** and 3,3'-bipyridinium.

3. Single Crystal X-Ray Crystallography

Data collections for **TTF⊂TBox-4^{2+}** was performed on a Rigaku XtaLAB PRO MM007 diffractometer equipped with a graphite monochromated Cu-Kα radiation (λ = 1.54184 Å). An absorption correction was applied using the SADABS program.[S4] The structures were solved by direct methods and refined on F^2 by full-matrix least-squares using the *SHELXTL*-97 program package.[S5] The ordered atoms in each structure were refined with anisotropic displacement parameters, while the hydrogen atoms were placed in idealized positions and allowed to ride on the relevant carbon atoms.

Crystal data for **TTF⊂TBox-4·2PF$_6$**: $C_{62}H_{50}F_{12}N_4O_{11}S_4P_2$, *Mr.* = 1445.24, monoclinic, space group $P2_1/c$, a = 12.5817(3) Å, b = 20.0466(4) Å, c = 25.8921(5) Å, α = γ = 90°, β = 93.079(10)°, V = 6521.1(2) Å^3, Z = 4, D_c = 1.380 g cm^{-3}, F_{000} = 2960, T = 180 (2) K, $2\theta_{max}$ = 130.3°, 54525 reflections collected, 11117 unique (R_{int} = 0.0788). *GooF* = 1.055, R_1 = 0.0583, wR_2 = 0.1415. CCDC-2307741 (**TTF⊂TBox-4·2PF$_6$**) contains the supplementary crystallographic data for this paper. These data can be obtained free of charge from The Cambridge Crystallographic Data Centre *via* www.ccdc.cam.ac.uk/data_request/cif. Because of the very large thermal motion and disorder of the solvents in the lattice, the diffuse residual electron density is difficult to be accurately modeled and thus a treatment by SQUEEZE (from PLATON) was used for solvate molecules, which leads to large solvent accessible voids in structures. Due to the same reason, the hydrogen atoms of solvent water molecules in the lattice were not located through diffuse residual electron densities.

4. Calculation of Photothermal Conversion Efficiency

4.1 TTF⊂TBox-1^{2+} aqueous solution

The conversion efficiency was determined according to the previous method.[S6, S7] The photothermal conversion efficiency (η) of **TTF⊂TBox-1^{2+}** was calculated by monitoring temperature change of **TTF⊂TBox-1^{2+}** in aqueous (2.7 mM) as a function of time under continuous laser irradiation (1064 nm, 1.5 W cm^{-2}) for 10 min (t). η was determined according to Equation (a):

$$\eta = \frac{hS(T_{max} - T_{surr}) - Q_{dis}}{I\left(1 - 10^{-A_{1064}}\right)} \qquad \text{(a)}$$

where h is heat transfer coefficient, S is the surface area of the container, T_{max} is the maximum system temperature (57 °C), and T_{surr} is ambient temperature of the surroundings (18.6 °C). Q_{dis} represents the heat dissipation from the light absorbed by the solvent and the quartz sample cell, I is the incident laser power (1.5 W cm^{-2}), and A_{1064} is the absorbance of the sample at 1064 nm (0.5576). The value of hS is obtained from Equation (b):

$$\tau_s = \frac{m_D c_D}{hS} \qquad \text{(b)}$$

where, m_D and c_D represent the mass (1.0 g) and heat capacity (4.2 J/g), respectively. τ_s is the time constant for heat transfer of the system, which is calculated from Equation (c):

$$t = -\tau_s \ln(\theta) = -\tau_s \ln\left(\frac{T - T_{surr}}{T_{max} - T_{surr}}\right) \qquad \text{(c)}$$

where, t is the cooling time points after continuous irradiation for 10 mins, T is the corresponding temperature of **TTF⊂TBox-1^{2+}** during the cooling stage, and according to Fig. 3c, τ_s is calculated to be 253.41 s. Based on Equation (b) and (c), the value of hS is determined to be 0.0166 W. Q_{dis} represents the heat dissipation from the light absorbed by the water and the container, which is determined according to Equation (d):

$$Q_{dis} = \frac{m_D c_D(T_{mas(water)} - T_{surr})}{\tau_{s(water)}} \qquad \text{(d)}$$

Where, $T_{max\ (water)}$ is 20.1 °C and τ_{water} is 249.3 s, thus Q_{dis} was determined to be 0.0252 W. According to the experiment data and Equation (a), η was calculated to be 56.3 %.

4.2 TTF⊂TBox-1²⁺ powders

The photothermal conversion efficiency of **TTF⊂TBox-1²⁺** was determined according to previous method.[S8] Details are as follows:

Based on the total energy balance for this system:

$$\sum_i m_i C_{p,i} \frac{dT}{dt} = Q_s - Q_{loss}$$

Where m_i (0.346 g) and $C_{p,i}$ (0.8 J (g °C)⁻¹) are the mass and heat capacity of system components (samples **TTF⊂TBox-1²⁺** and quartz glass), respectively. The mass of samples **TTF⊂TBox-1²⁺** is negligible compared with that of quartz glass, the heat capacity of quartz glass is therefore used for photothermal conversion efficiency calculation of samples **TTF⊂TBox-1²⁺**. Q_s is the photothermal heat energy input by irradiating NIR laser to samples **TTF⊂TBox-1²⁺**, and Q_{loss} is thermal energy lost to the surroundings. When the temperature is maximum, the system is in balance.

$$Q_s = Q_{loss} = hS\Delta T_{max}$$

where h is heat transfer coefficient, S is the surface area of the container, ΔT_{max} is the maximum temperature change. The photothermal conversion efficiency η is calculated from the following eaquation:

$$\eta = \frac{hS\Delta T_{max}}{I\left(1 - 10^{-A_{808}}\right)}$$

where I is the laser power (0.6 W cm⁻²) and A_{808} is the absorbance of the samples at the wavelength of 1064 nm (0.206).

In order to obtain the hS, a dimensionless driving force temperature, θ is introduced as follows:

$$\theta = \frac{T - T_{surr}}{T_{max} - T_{surr}}$$

where T is the temperature of samples **TTF⊂TBox-1²⁺**, T_{max} is the maximum system temperature (83 °C), and T_{surr} is the initial temperature (24.0 °C).

The sample system time constant τ_s

$$\tau_s = \frac{\sum_i m_i C_{p,i}}{hS}$$

then

$$\frac{d\theta}{dt} = \frac{1}{\tau_s} \frac{Q_s}{hS\Delta T_{max}} - \frac{\theta}{\tau_s}$$

when the laser is off, $Q_s = 0$, therefore $\frac{d\theta}{dt} = -\frac{\theta}{\tau_s}$, and $t = -\tau_s \ln \theta$

So hS could be calculated from the slope of cooling time vs ln θ. Therefore, τ_s is 90.0 s (Fig. S4) and the photothermal conversion efficiency η is 80.1%.
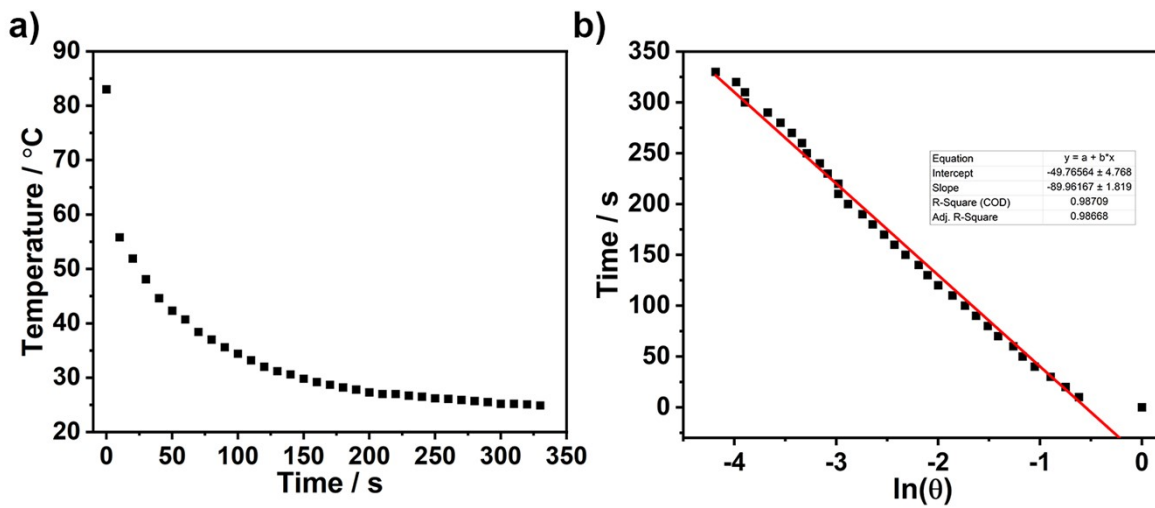

Fig. S7. a) The cooling curve after the irradiation of 1064 nm laser (0.6 W cm^{-2}) and b) the corresponding time-lnθ linear curve of **TTF⊂TBox-1^{2+}**.
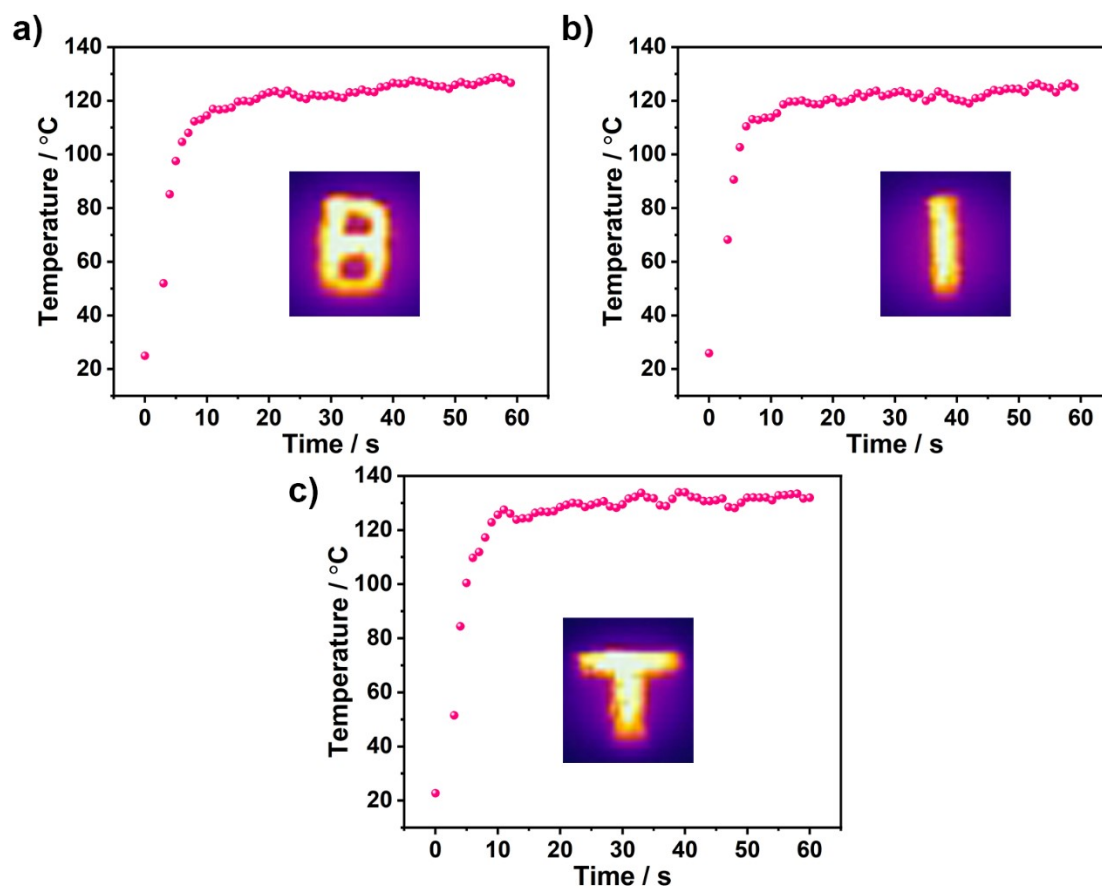
5. Photothermal Imaging of TTF⊂TBox-1²⁺ Powders

Fig. S8. The photothermal conversion curves over time of PT imaging.

6. Calculation of Water Evaporation Efficiency

The water evaporation efficiency was determined according to the previous method.[S9] The water evaporation rate was calculated by the following equation:

$$v = \frac{dm}{S \times dt}$$

Where m is the mass of evaporated water, S is the illuminated area, t is time, and v is evaporation rate.

In the end, Light to water evaporation efficiency (η) was calculated based on following equation:

$$Q_e = \frac{dm \times H_e}{dt} = v \times H_e$$

$$\eta = \frac{Q_e}{Q_s}$$

Where Q_e is energy consumed for water evaporation, Q_s is the incident simulated solar light power (2500 W/m^2), m is the mass of evaporated water recorded by the balance, and H_e is the enthalpy of vaporization of water (2266 kJ/kg).

Table S1 Light to water Evaporation efficiency of the control experiments

	Evaporation rate (kg m^{-2} h^{-1})	Evaporation efficiency
The PTFE membrane	0.66	16.6%
TTF⊂TBox-1^{2+}-PTFE membrane	2.25	56.6%

7. References

[S1] F. Yang, C. Liu, D. Yin, Y. Xu, M. Wu, W. Wei, *Chem. Commun.*, 2019, **55**, 14335-14338.

[S2] H. Cong, L.-L. Tao, Y.-H. Yu, Z. Tao, F. Yang, Y.-J. Zhao, S.-F. Xue, G. A. Lawrance and G. Wei, *J. Phys. Chem. A.,* 2007, **111**, 2715-2721.

[S3] F. Yang, Y. Li, R. Li, X. Wang, X. Cui, W. Wei and Y. Xu, *Org. Chem. Front.*, 2022, **9**, 2902-2909.

[S4]. G. M. Sheldrick, SADABS: Program for Empirical Absorption Correction of Area Detector Data; University of Göttingen, Göttingen, Germany, 1996.

[S5]. G. M. Sheldrick, SHELXL-97, Program for Solution of Crystal Structures, University of Göttingen, Göttingen, Germany, 1997.

[S6]. S. Tian, H. Bai, S. Li, Y. Xiao, X. Cui, X. Li, J. Tan, Z. Huang, D. Shen, W. Liu, P. Wang, B. Z. Tang and C. S. Lee, *Angew. Chem., Int. Ed.*, 2021, **60**, 11758-11762.

[S7]. X. Li, L. Liu, S. Li, Y. Wan, J. X. Chen, S. Tian, Z. Huang, Y. F. Xiao, X. Cui, C. Xiang, Q. Tan, X. H. Zhang, W. Guo, X. J. Liang and C. S. Lee, *ACS Nano.*, 2019,**13**, 12901-12911.

[S8] Y. Wang, W. Zhu, W. Du, X. Liu, X. Zhang, H. Dong, W. Hu, *Angew. Chem., Int. Ed.*, 2018, **57**, 3963-3967.

[S9] D. Wang, X. Kan, C. Wu, Y. Gong, G. Guo, T. Liang, L. Wang , Z. Li, Y. Zhao, *Chem. Commun.*, 2020, **56**, 5223-5226.